Adaptive Control Strategies for Open-loop Dynamic Hopping

Marco Hutter, C. David Remy, and Roland Siegwart, *Fellow, IEEE*

Abstract— In the present study, we investigate a control strategy for hopping motions of an articulated leg that is driven by series elastic actuation. A highly compliant spring in the knee joint allows the exploitation of periodic energy storage but creates a major control challenge by severely limiting the bandwidth of closed-loop position or force control. This handicap is intensified by slow actuators, substantial delays, and the kinematic coupling of the articulated design.

With classic closed-loop control strategies failing, an adaptive open-loop control algorithm is presented, that, over a series of jumps, estimates the compression of the actuator springs, and gradually modifies the motor inputs in order to minimize slipping and create a purely vertical motion.

I. INTRODUCTION

RUNNING gaits of humans and animals are characterized by a vertical oscillation of the center of mass on springy legs with a periodic exchange of potential, kinetic, and elastic energy [1]-[3]. During ground contact, elasticities in muscles and tendons temporarily store energy which is recovered later in the gait cycle, thereby yielding a very efficient motion. This basic principle has long found its way into robotics, where the energy is stored in springs [2], [4], [5] or pneumatic pistons [6] in a number of robotic leg designs with prismatic [6]-[9] or articulated structure [10]-[12]. The use of low stiffness springs in this context, allows for an expanded ground phase which is beneficial for postural control and reduces the power requirements of the actuators as more time is granted to feed energy into the system [3], [13]. If the actuators are used to move the neutral positions of the springs (Fig. 1) this control and activation can be performed without impeding the natural dynamic motion at all. The effective joint torque τ produced by such a system is a function of the joint angle γ and the actuator angle φ, as well as their respective velocities $\dot{\gamma}$ and ω:

$$\tau = c \cdot (\gamma - \varphi) + d \cdot (\dot{\gamma} - \omega) = c \cdot \delta + d \cdot \dot{\delta} \qquad (1)$$

(with the spring constant c and the damping coefficient d). This is referred to as *series elastic actuation* [14], [15],
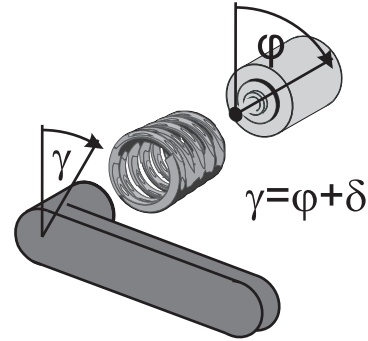
Fig. 1. In a series elastic actuator a compliant element decouples the joint from the actual actuator.
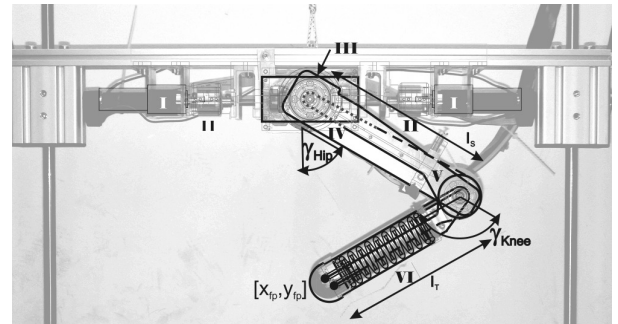

Fig. 2. Experiments were performed on an articulated robotic leg with series-elastic actuation. The spring for knee actuation was included in the shank and connected to the hip motor with a cable pulley system.

although in this context the spring is not used as a force-controllable element, but as an integral dynamic component of the mechanical system. The disadvantage of this actuator structure is that the compliant element acts as a mechanical low-pass filter, which severely limits the bandwidth of the control of joint angles γ or joint angle velocities $\dot{\gamma}$ [16].

To investigate the benefit of elastic energy storage in passive dynamic running, we built an articulated leg with series-elastic actuation in the hip and knee joints, and developed control algorithms for one dimensional hopping. We decided to use an articulated design, as it has been shown that the nonlinear relationship between leg compression and leg stiffness of an articulated leg has a beneficial impact on open loop stability and can increase the range of stable running speeds [17] in comparison to a prismatic leg with a linear compression-stiffness ratio. Additionally, the dynamics of an articulated leg can perform a passive swing leg retraction and the larger range of motion increases the achievable ground clearance [18]. However, controlling a hopping motion becomes more complicated due to the nonlinear kinematic coupling of the joints.
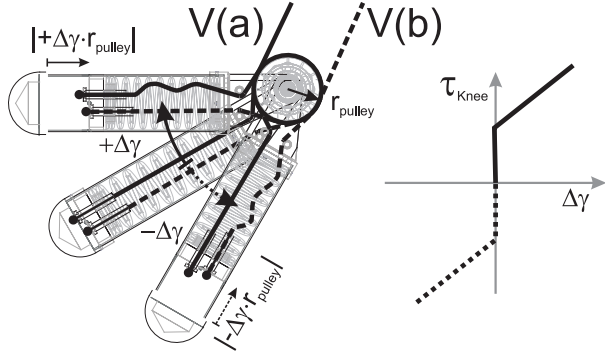
Fig. 3. A pulley system in combination with a single pre-compressed spring for knee flexion and extension resulted in a nonlinear spring-characteristic at joint level, which substantially increased the damping for the unloaded leg.

The focus of our work was on the creation of adaptive open-loop control strategies that circumvent the low bandwidth dilemma (which is worsen by large delays in our control system) by considering the control task not as a time continuous problem, but on a step-to-step basis. Open-loop trajectories for the hip and knee motor angles $\left(\varphi_{Hip}/\varphi_{Knee}\right)$ and velocities $\left(\omega_{Hip}/\omega_{Knee}\right)$ were used to generate attractive limit cycles for the joint angles γ_{Hip} and γ_{Knee} that resulted in a purely vertical hopping motion without slipping during ground contact. The ability to accurately shape the underlying limit cycle is the base for extending the lineal motion to planar (or even 3D) hopping while exploiting the advantages of the passive spring dynamics in the actuators [19]-[21].

II. METHODS

The robotic leg used in this project (Fig. 2) consists of three segments (main body, shank, and thigh) that are driven by two series-elastic hip actuators (motors (I), springs (II)) connected by a differential drive for hip flexion/extension, as well as abduction/adduction, and a knee motor (III) that is linked over a miniature chain drive (IV) and a cable pulley system (V) with the highly compliant knee spring (VI) in the shank for series elastic knee flexion/extension. As the cable pulleys for knee-flexion (Fig. 3, V(a)) and for knee extension (Fig. 3, V(b)) are attached to the same side of the spring, the spring is only used in one direction, namely compression. Hence, pre-compression of this system (by tensioning the pulley system) leads to a nonlinear spring characteristics, which yield low damping if the leg is loaded and very high damping if it is unloaded, allowing open loop positioning of the joint during flight [22]. For the presented study, the main body was restricted to pure vertical motion and the hip abduction/adduction was blocked, resulting in a system with three degrees of freedom.

Three separate controller phases were defined for stance [A], flight [B], and pre-impact speed matching [C] (Fig. 4). Transitions between these phases were based exclusively on motor and knee angle encoder states.
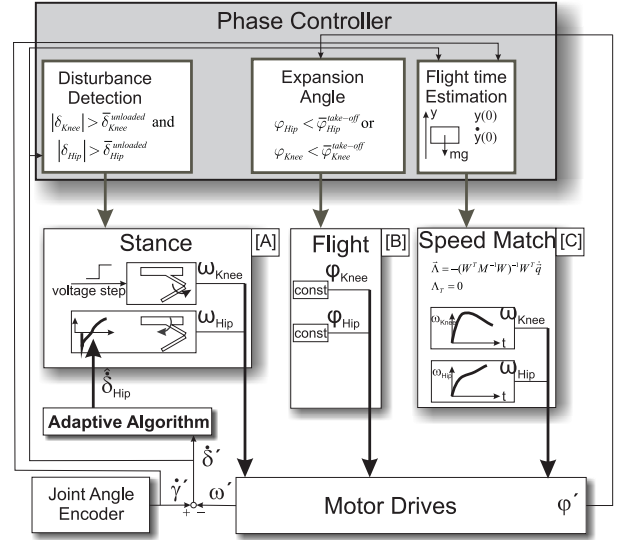

Fig. 4. A three-phase open-loop control strategy generated motor trajectories for stance, flight, and pre-impact speed matching.

Stance: During the stance phase, the basic hopping motion was generated by thrusting the knee motor with a desired angular velocity $\overline{\omega}_{Knee}^{desired}$. The hip motor speed profile ω_{Hip} was set to ensure a purely vertical motion of the ground contact point $\left(\dot{x}_{fp}(t)\equiv 0\right)$ and thus prevent slipping of the foot. In terms of joint angles this can be expressed as:

$$\dot{x}_{fp} = l_T \cos\left(\gamma_{Hip}\right)\dot{\gamma}_{Hip} - l_S \cos\left(\gamma_{Knee}-\gamma_{Hip}\right)\left(\dot{\gamma}_{Knee}-\dot{\gamma}_{Hip}\right)\equiv 0 \quad (2)$$

When using this equation to generate control inputs for the hip motor, one has to account for the compression δ in the springs of the series elastic actuators:

$$\dot{\gamma}_{Hip} = \omega_{Hip} + \dot{\delta}_{Hip}$$
$$\dot{\gamma}_{Knee} = \omega_{Knee} + \dot{\delta}_{Knee} \quad (3)$$

As a closed loop implementation of equations (2) and (3) was impossible due to the substantial delays in the control system, open loop trajectories for $\omega_{Hip}(t)$ were generated based on estimates $\hat{\delta}(t)$ of the spring compression. An adaptation scheme updated these estimates with the current measurement $\dot{\delta}'(t)$ after every jump:

$$\hat{\dot{\delta}}_{Hip}^{k+1}(t) = (1-k)\cdot\hat{\dot{\delta}}_{Hip}^{k}(t) + k\cdot\dot{\delta}'_{Hip}(t)$$
$$\hat{\dot{\delta}}_{Knee}^{k+1}(t) = (1-k)\cdot\hat{\dot{\delta}}_{Knee}^{k}(t) + k\cdot\dot{\delta}'_{Knee}(t) \quad (4)$$

To generate an initial estimate, we assumed zero spring compression $\hat{\delta}^0(t)\equiv 0$ and subsequently simulated a

simplified adaptation without actuator dynamics which then served as a base for all further studies. The update factor k defines the weighted ration between the old estimate and the current measurement, thus influencing the convergence rate and robustness of the algorithm.

Using the estimated spring compression to predict the knee joint angle of the subsequent expansion phases $\left(\hat{\gamma}_{Knee}^{k+1} = \omega_{Knee} + \hat{\delta}_{Knee}^{k+1} \right)$, leads to an ordinary differential equation for the required hip joint angle $\hat{\gamma}_{Hip}^{k+1}$:

$$\hat{\gamma}_{Hip}^{k+1} = \frac{l_s \cos\left(\hat{\gamma}_{Knee}^{k+1} - \hat{\gamma}_{Hip}^{k+1} \right) \hat{\gamma}_{Knee}^{k+1}}{l_T \cos\left(\hat{\gamma}_{Hip}^{k+1} \right) - l_s \cos\left(\hat{\gamma}_{Knee}^{k+1} - \hat{\gamma}_{Hip}^{k+1} \right)} \tag{5}$$

By integrating this equation, the hip motor trajectory for the following jump was calculated:

$$\omega_{Hip}^{k+1} = \hat{\gamma}_{Hip}^{k+1} - \hat{\delta}_{Hip}^{k+1} \tag{6}$$

One should note that it is not necessary to obtain an absolute precise estimation of the spring compressions δ. The friction force between ground and foot affects the dynamics of the system, such that equation (2) will hold, even if the motor trajectories $\omega_{Hip}(t)$ are not entirely correct.

The transition to the flight phase of the controller is initiated by thresholds in the actuator positions:

$$\varphi_{Hip} < \overline{\varphi}_{Hip}^{take-off} \text{ or } \varphi_{Knee} < \overline{\varphi}_{Knee}^{take-off} \tag{7}$$

One should note that this transition condition does not necessarily mean that the leg actually left the ground. As the normal ground contact force can not be considered in the transition detection, it is possible that the leg is still on the ground. However, from this point on, no further energy is fed into the system and the actual take-off will happen purely passively.

Flight: During flight, the leg is simply brought into a predefined landing configuration where it is awaiting touch down:

$$\gamma_{Hip} = \overline{\gamma}_{Hip}^{flight}, \gamma_{Knee} = \overline{\gamma}_{Knee}^{flight}, \dot{\gamma}_{Hip} = \dot{\gamma}_{Knee} = 0 \tag{8}$$

Again, it is impossible to establish direct closed loop control of the desired joint angles. The natural dynamics of the unloaded leg are too fast and can not be manipulated with the low-bandwidth actuators. Fortunately, the nonlinear series elastic knee design used in this study provides very high damping if the leg is unloaded [22], which allowed precise leg positioning by simply setting the actuator position

to the desired joint angles:

$$\varphi_{Hip} = \overline{\gamma}_{Hip}^{flight}, \omega_{Hip} = 0$$
$$\varphi_{Knee} = \overline{\gamma}_{Knee}^{flight}, \omega_{Knee} = 0 \tag{9}$$

Transition to the speed phase was based purely on the elapsed time since take-off and happens shortly before impact:

$$t > \overline{t}^{flight} - \varepsilon \tag{10}$$

The timing of this transition is critical. It ensures that both, velocity and position of the impacting leg are in the appropriate value range at touch down. The expected flight time $\overline{t}^{flight}$ was estimated through a simplified model that is provided with the system states at lift-off. The timing variable ε defines the duration of the speed matching phase. It provides time to adequately accelerate the segments prior to impact and was chosen according to the dynamic capabilities of the actuators.

Pre-impact speed matching: The instantaneous changes in velocity due to the collision at touch down pose an additional control challenge. For all feasible angle configurations of the landing leg, the collision generates a tangential impulsive force that leads to a non-zero velocity component $\dot{x}$ of the contact point right after touch-down. Compensating this motion to prevent slipping, requires instantaneous changes in the hip motor velocity ω_{Hip} which can not be generated with real actuators. This would make it impossible that the adaptive algorithm converges in the real system, or in a simulation that models motor dynamics.

Again, an open loop strategy provides the solution: Shortly before touch-down, the leg segments are accelerated to designated pre-impact velocities, which eliminate the tangential impulse Λ_T of the contact collision. Without a horizontal impulse component, no slipping occurs, and the contact point remains at rest after impact. The necessary pre-impact velocities are calculated with a plastic collision model [23]:

$$\vec{\Lambda} = [\Lambda_N, \Lambda_T]^T = -(W^T M^{-1} W)^{-1} W^T \dot{\vec{q}}^- \tag{11}$$

The impulsive forces at impact $\vec{\Lambda}$ depend on the pre-impact velocities $\dot{\vec{q}}^-$, and the mass matrix $M(\vec{q})$. They can be expressed in generalized coordinates $\vec{q} = [y, \gamma_{Hip}, \gamma_{Knee}]^T$ by using the generalized normal and tangential force directions $W = [\vec{w}_N(\vec{q}), \vec{w}_T(\vec{q})]$. When setting the tangential impulse to zero, an ordinary differential equation results $\left(\Lambda_T(\vec{q}(t), \dot{\vec{q}}(t)) = 0 \right)$ that can be solved for $\gamma_{Hip}(t)$ and
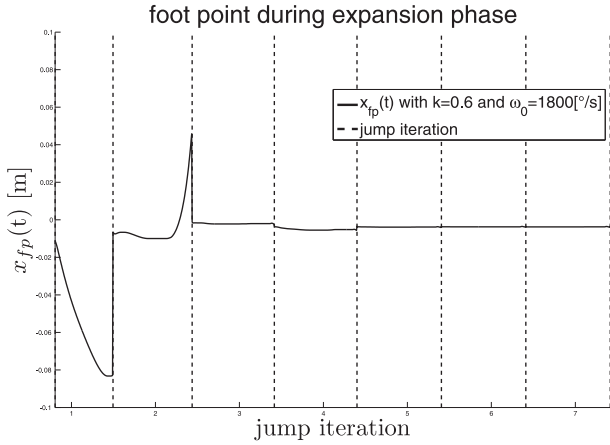
Fig. 5. Evolution of the horizontal foot point trajectory during the simulation of consecutive expansion cycles. By iteratively adapting the speed of the hip motor, the unwanted horizontal motion is eliminated within three speed profile adaptation iterations.

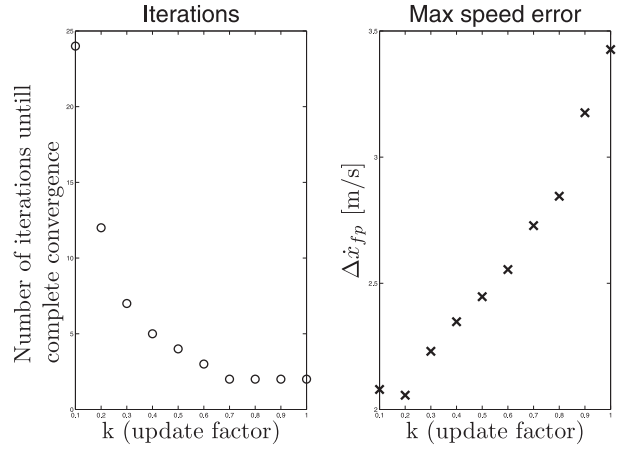

Fig. 6. The convergence rate of the algorithm (a) can be adjusted by the update factor k. Higher factors led to faster convergence but introduced higher horizontal speed errors (b) during the adaptation. The presented results were produced in simulation.

$\gamma_{Knee}(t)$ starting with the landing configuration $\overline{\gamma}_{Hip}^{flight}$ and $\overline{\gamma}_{Knee}^{flight}$, and an estimated downward speed $\dot{y}^-$ before impact. As this poses only one constraint for two degrees of freedom $\left(\dot{\gamma}_{Hip}, \text{ and } \dot{\gamma}_{Knee} \right)$ we additionally minimize the velocity of the foot point $\left| \vec{v}_{fp} \right| = \sqrt{\dot{x}_{fp}^2 + \dot{y}_{fp}^2}$. This computation can be performed off-line as all necessary quantities are known beforehand. The resulting velocity trajectories are used directly as actuator setpoints φ_{Hip} and φ_{Knee}. Due to the high damping in the series elastic actuator, the joint angles γ_{Hip} and γ_{Knee} follow automatically.

Touch-down is detected by observing a compression of the spring in the hip actuator δ_{Hip} or the knee actuator δ_{Knee}:

$$\left| \delta_{Knee} \right| > \overline{\delta}_{Knee}^{unloaded} \text{ or } \left| \delta_{Hip} \right| > \overline{\delta}_{Hip}^{unloaded} \qquad (12)$$

If both compressions exceed a certain threshold value we assume, that the leg is not longer unloaded and that ground contact was established. The controller phase is set to stance.

The controller described above was first implemented in a detailed simulation of the monopod leg that included the multi body dynamics, intermitted ground contact, actuator dynamics, frictional effects, and all other limitations of the digital control system - including discrete sampling, delays, and power limitations. The unilateral contact between foot and ground was formulated and implemented as a linear complementary problem [24] and included slipping and Coulomb friction. The equations of motion were derived using projected Newton-Euler equations [25]. They were implemented and integrated using MATLAB/Simulink [26]. Simulations were performed for different load scenarios, knee expansion speeds $\overline{\omega}_{Knee}^{desired}$, and friction coefficients. The convergence of the algorithm was studied for varying

values of the update factor *k*.

In subsequent experiments, the actuator inputs generated in simulation were used to drive the motors of the actual prototype to show the practicality of the approach. I.e., the pre-computed trajectories of stance and flight phase were executed open-loop without using sensory feedback other than for detecting phase transitions. At this stage the necessary sensing capabilities were missing at the hip joint of the actual prototype to fully implement the adaptation algorithm, but the agreement of the resulting limit cycles in simulation and open-loop experiment still served as an indicator that the algorithm could be executed directly on the prototype. For the same reason, we had to restrict ourselves to the implementation of the stance and flight phases and disable speed matching in the actual robot. However, by using a relatively soft ground surface with a high coefficient of friction, we could limit the slipping at ground contact to a negligible amount that didn't affect the performance of the hopper.

III. RESULTS

In the detailed simulation, the presented algorithm converged robustly towards a purely vertical, open-loop jumping motion without slipping (Fig. 5). A steady limit cycle was reached within less than 4 jumps. The rate of convergence depended on the update factor *k* that weighted the current estimate of the spring compression $\hat{\dot{\delta}}^k(t)$ against the most recent measurement $\dot{\delta}'(t)$. Smaller update factors correspond to a more conservative algorithm. A higher number of jumps were required for convergence, but the residual foot motion (slipping) during the adaptation phase was reduced. Additionally, the algorithm is more robust to measurement errors or disturbances. We achieved best results with an update factor of *k* = 0.6 (Fig. 6).

Smooth motor trajectories for hip and knee were generated for different desired knee expansion speeds $\overline{\omega}_{Knee}^{desired}$ which
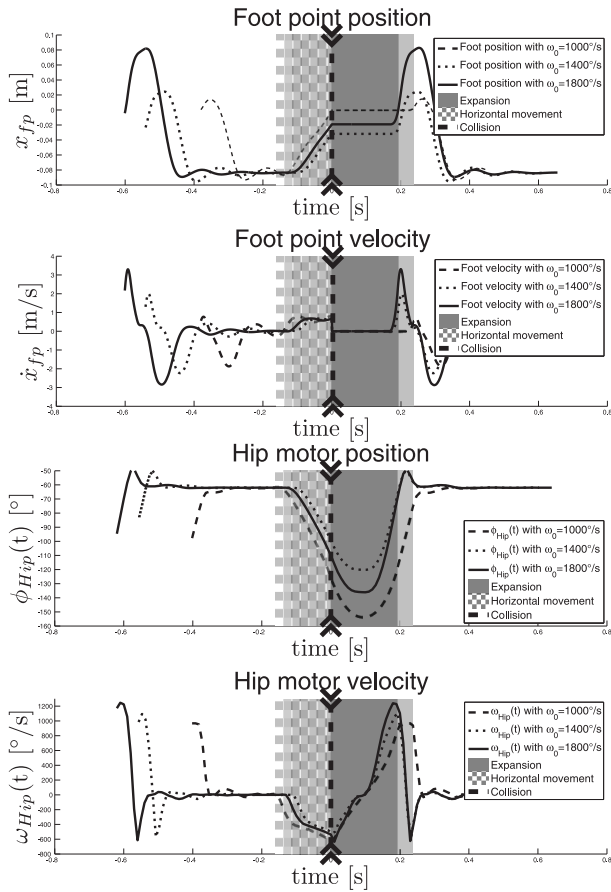
Fig 7. Horizontal foot point motion (a) and hip motor trajectories (b) for the simulation of a complete hopping-cycle. Results are shown for three different knee-thrusting speeds.

Fig. 8. Knee joint angle and angular velocity in a series of consecutive jumps show good agreement of simulation and experiment.

allowed accurate adjustment of the jumping height and adaptation to different load scenarios. A series of such motor trajectories is presented in Fig. 7.

The detailed simulation was compared with experiments performed on the actual prototype and showed excellent agreement. The adapted trajectories from the simulated 2-phase algorithm were directly used as an input for both simulations and experiments using the presented hardware. Even when started with different initial conditions, motor ($\phi_{Hip}(t), \phi_{Knee}(t)$) and joint angles ($\phi_{Knee}(t)$) from simulation and experiments converged to a limit cycle with very close agreement (Fig. 8).

The full 3-phase controller in a simulation with uneven ground suffered from the inexact knowledge about flight time. Without sufficient time for acceleration prior to landing, it is impossible to avoid the tangential impulse during the collision with the ground, resulting in unwanted slipping. Apart from this problem, the other two phases of the controller (e.g. in the experiments with the soft ground surface) showed very high robustness against variations in ground height. The landing posture is reached quickly after lift-off, allowing a large variation of the ground height during flight. Additionally, the resulting limit cycle is robust against disturbance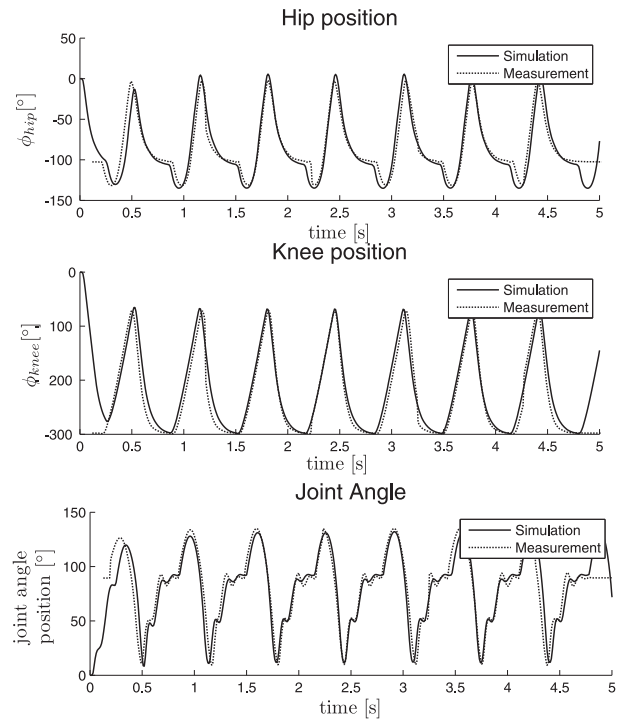s, which means that constant actuator expansion trajectories during stance phase will bring the leg back on the desired limit cycle within 2 consecutive jumps.

IV. DISCUSSION

A three phase open-loop control strategy for passive dynamic hopping with highly compliant series elastic actuation and kinematic coupling was successfully implemented and tested in simulations and experiments of an articulated robotic leg. The controller adaptively generated open-loop motor trajectories for stance, flight, and pre-impact speed matching. These trajectories resulted in stable limit cycles and enabled periodic hopping for different loads and height levels. Simulation based trajectory generation was possible on the basis of a very accurate model.

A key element in the leg design is the pulley system in the elasticity of the knee actuator. The nonlinear spring characteristic in combination with internal collisions of the uni-directional spring substantially increased the damping of the unloaded leg and allowed open-loop positioning while the leg was in the air. If the leg is loaded, however, the spring is operated in its linear range without crossing its neutral position and energy losses are minimized.

Series elastic actuation with highly compliant elastic elements is a promising approach to add actuation to otherwise purely passive dynamic (and hence very efficient) systems. Low spring stiffnesses are necessary to match the stride frequency of the running gait with the natural dynamics of the actuators in order to enable optimal energy recovery [27]. This allows the use of smaller and slower actuators, but poses a severe control challenge as classic

closed-loop control on joint level becomes impossible.

Instead of enforcing continuously controlled joint angles, we believe in open-loop strategies that merely shape dominantly passive limit cycles [28]. To this end, strategies must be developed that allow the generation (and adaptation) of the necessary actuator inputs. In this paper, a set of such strategies is presented for the archetype of all running gaits - one-dimensional periodic hopping [29]. Even though, this is an extremely coarse approximation of an actual bipedal or quadrupedal running motion, the fundamental issues of high-compliance series elastic actuation remain the same: The actual motion can never be precisely shaped or even predicted. However, as it can be assumed (or is at least the goal for steady state running) that the motion is periodic, adaptations can be made on a stride to stride basis. In this example the alterations are made to ensure a purely vertical motion of the robot's foot and prevent slipping during stance and landing, but the same methods can be used to enforce a desired angle of attack in planar or 3D hopping, or control the attitude of the hopper during stance before extending them to multi-legged robots.

In our project we are now aiming towards two extensions: Firstly we want to equip the robotic prototype with adequate sensing capabilities at the hip actuator spring to be able to run the entire algorithm online. This is important to ensure convergence in the experimental setup and study how robust the algorithm is to actual disturbances or changes in the system configuration. In the design progress we aim at augmenting the system with a foot element that passively acts as a third leg segment. A precise selection of length and mass properties of this segment avoids tangential impulse at landing even without using the speed matching algorithm. This increases the robustness against terrain height disturbances on non-compliant ground surfaces.

REFERENCES

[1] G. A. Cavagna, F. P. Saibene, and R. Margaria, "Mechanical work in running," *Journal of Applied Physiology*, 19 (2), 1964, pp. 249-256.

[2] G. A. Cavagna, N. C. Heglund, and C. R. Taylor, "Mechanical Work in terrestrial locomotion: two basic mechanisms for minimizing energy expenditure, "*American Journal for Physiology*, 233 (5), 1977, pp. 243-261

[3] C. T. Farley, J. Glasheen, and T. A. McMahon, "Running springs: speed and animal size, "*Journal of Experimental Biology*, 185, 1993, pp. 71-86

[4] M. H. Dickinson, C. T. Farley, R. J. Full, M. A. Koehl, R. Kram, and S. Lehman, "How animals move: an integrative view," *Science*, 288 (5463), 2000, pp. 100-106

[5] T. Luksch, K. Berms, and F. Flörchinger, "System and Control Concept for a Running Biped," in *Fast Motions in Biomechanics and Robotics,* Springer, Berlin, 2007., pp. 219-231.

[6] M. H. Raibert, *Legged Robots that balance,* MIT Press, Cambridge Massachusetts, 1986.

[7] M. Ahmadi, and M. Buehler, "Stable control of a Simulated One-Legged Running Robot with Hip and Leg Compliance", *IEEE Transactions on Robotics and Automation,* 13, 1997, pp. 96-104

[8] P. Gregorio, M. Ahmadi, and M. Buehler, "Experiments with an Electrically Actuated Planar Hopping Robot", in *Experimental Robotics III,* Springer, 1994, pp. 269-281

[9] H. D. Taghirad, "Analysis, Design, and Control of a Hopping Robot," M. Eng. *Project Report*, Department of Mechanical Engineering, McGill University, Montreal, Canada, 1993

[10] L. R. Palmer, D. E. Orin, D. W. Marhefka, J. P. Schmiedeler, and K. J. Waldron, "Intelligent Control of an Experimental Articulated Leg for a Galloping Machine," in *Proc. IEEE International Conference on Robotics and Automation*, Taipei, Taiwan, 2003

[11] H. DeMan, D. Lefeber, and J. Vermeulen, "Design and control of a robot with one articulated leg for locomotion on irregular terrain," in *Proc. of the Twerlfth CISM-IFToMM Symposium on Theory and Practice of Robots and Manipulators*, Vienna, Springer, 1998, pp. 417-424

[12] S. Curran, and D. E. Orin, "Evolution of a Jump in an Articulated Leg with Series-Elastic Actuation," *IEEE International Conference on Robotics and Automation*, Pasadena, CA, USA, 2008

[13] A. Seyfarth, H. Geyer, M. Günther, and B. Reinhard, "A movement criterion for running," *Journal of Biomechanics*, 35, 2002

[14] J. E. Pratt, and B. T. Krupp, "Series Elastic Actuators for legged robots," in *Proc. The international Society for Optical Engineering*, 5422, 2004, pp. 135-144.

[15] D. W. Robinson, "Design and Analysis of Series Elasticity in Closed-loop Actuator Force Control," *PhD Thesis*, Department of Mechanical Engineering Massachusetts Institute of Technology (MIT), 2000

[16] G. A. Pratt, and M. M. Williamson, "Series Elastic Actuators", in *Proc. IEEE/RSJ Int. Conf. on Intelligent Robots and Systems (IROS),* Pittsburg, 1995, pp. 399-406

[17] J. Rummel, and A. Seyfarth, "Stable Running with Segmented Legs," *The International Journal of Robotics Research,* 27, 2008

[18] S. H. Hyon, R. Mita, "Development of a biologically inspired hopping robot-'Kenken'," in *Proc. IEEE International Conference on Robotics and Automation*, Washington DC, USA, 2002

[19] R. Blickhan, "The spring-mass model for running and hopping," *Journal of Biomechanics,* 22(11-12), 1989, pp. 1217-1227

[20] T. A. McMahon, and G. C. Cheng, "The mechanics of running: how does stiffness couple with speed?," Journal of Biomechanics, 23(1), 1990, pp. 65-78

[21] W. J. Schwind, and D. E. Kodischek, "Characterization of monoped equilibrium gaits," in *Proc. of the IEEE International Conference on Robotics and Automation*, Albuqerque, NM, 1997, pp. 1986-1992

[22] M. Hutter, C. D. Remy, and R. Siegwart, "Design of an Articulated Robotic Leg with Nonlinear Series Elastic Actuation", in *Proc. Of international Conference on Climbing and Walking Robots*, Istanbul, Turkey, 2009

[23] C. Glocker, "Dynamik von Starrkörpersystemen mit Reibung und Stössen," in *VDI-Fortschrittsberichte Mechanik/Bruchmechanik*, VDI-Verlag, Düsseldorf, 1995, pp. 97-132

[24] F. Pfeiffer, and C. Glocker, *Multibody Dynamics with Unilateral Contacts*, John Wiley & Sons, New York, 1996

[25] C. Glocker, *Set-Valued Force Laws: Dynamics of Non-Smooth Systems*, Springer, Berlin, Heidelberg 2001

[26] L. F. Shapine, and M. W. Reichelt, "The MATLAB ODE suite," *SIAM Journal on Scientific Computing.*, 18, 1997, pp. 1-22

[27] C. T. Farley, R. Blickhan, J. Saito, and C. R. Taylor, "Hopping frequency in humans: a test of how springs set stride frequency in bouncing gaits," *Journal of Applied Physiology*, 71, 1991

[28] J. G. Cham, and M. R. Cutkosky, "Dynamic Stability of Open-loop Hopping," *Journal of Dynamic Systems, Measurement, and Control,* 129, 2007

[29] M. H. Raibert, *Legged Robots*, Commun. ACM, 29, New York, USA, 1986 pp. 499-514

V. ACKNOWLEDGEMENTS